Sub-micron Scaling of High-Speed InP/InGaAs SHBTs Grown by MOCVD using Carbon as the p-Type Dopant

M.L. Hattendorf, Q.J. Hartmann*, K. Richards*, and M. Feng

Department of Electrical and Computer Engineering · University of Illinois
Microelectronics Laboratory · 208 N. Wright Street · Urbana, IL 61801
Phone: **(217) 333-4055**, e-mail: **mhattend@students.uiuc.edu**

*Epiworks, Inc. · 1606 Rion Drive · Champaign, IL 61822

Abstract

InP-based single heterojunction bipolar transistors (SHBTs) are being actively investigated for 40 Gbps fiber-optic applications. In this work, we report the fabrication of high-speed sub-micron SHBTs grown by MOCVD with 2×10^{19} cm^{-3} Carbon as the p-type dopant. Graded-base technology and aggressive lateral scaling are used to improve RF performance.

INTRODUCTION

InP-based single heterojunction bipolar transistors (SHBTs) are being actively investigated for 40 Gbps fiber-optic applications. Transistors in this material system have demonstrated high-speed capability and allow monolithic integration of detectors with HBTs. Devices with Carbon doping in the base show superior reliability characteristics relative to devices with Beryllium doping. [1] Most research on Carbon-doped InP/InGaAs HBTs has focused the Molecular Beam Epitaxy (MBE) techniques [2, 3], although recent work has also investigated Metal-Organic Chemical Vapor Deposition (MOCVD) [4].

The wide-bandgap emitter of an HBT allows the fabrication of transistors with a simultaneously large DC current gain and base doping level. A large base doping level in turn allows for the realization of thin bases with low sheet resistance for high-speed operation. However, the base doping level may be limited in practical devices by crystal growth issues or reliability concerns. For example, the active dopant concentration in the base of a Carbon-doped InP/InGaAs HBT grown by MOCVD is often relatively low because of Hydrogen passivation. [5] Various techniques have been demonstrated to improve RF performance in InP/InGaAs HBTs at a fixed doping level. This paper is primarily concerned with one such technique: lateral scaling

There are two major reasons to decrease the lateral dimensions of an HBT. The first of these is to decrease the power consumption of a transistor [6], and the second is to improve high-frequency performance. To a first order approximation, current gain cutoff frequency f_T, is expected to be independent of device size, while power gain cutoff frequency f_{MAX} is expected to be inversely proportional to the square-root of emitter width in a standard stripe-geometry HBT. Research on transferred-substrate HBTs has demonstrated the potential benefits of this lateral scaling [7], but there has not been very much work exploring benefits of scaling on RF performance in standard double-mesa HBTs. This lack has been attributed by researchers to various causes, such as difficulties managing parasitics in small devices [6] and concerns about ohmic contact transfer length for the base electrode. [7] This work demonstrates that scaling is an effective technique to improve high-speed performance in standard double-mesa HBTs.

GROWTH

A simple parameter to quantify the quality of base material is the ratio of dc current gain β to base sheet resistance R_{SB}. For a given base thickness, this ratio can be optimized by adjusting various growth conditions, including V / III ratio, growth temperature, extrinsic dopant source CCl_4 flow, and anneal conditions. A relatively low base R_{SB} can be achieved while maintaining an adequate DC current gain β at the 2×10^{19} cm^{-3} doping level. However, due to the diffusive nature of electron transport in InGaAs, the β to R_{SB} ratio decreases as base thickness increases, as shown in Fig. 1.

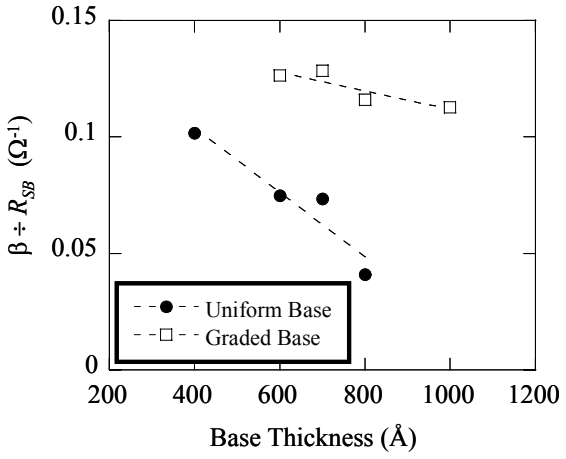

Fig 1. β ÷ R_{SB} as a function of base width for uniform and graded bases.

The falloff in β÷RSB with base thickness is a problem for high-speed applications which require an adequate β yet benefit from a minimum R_{SB}. To address this problem, a graded base growth technique was developed. Since a graded base accelerates electrons through the base, it is reasonable to assume that the speed performance of a graded base will be comparable to a thinner, non-graded base. Figure 1 shows a dramatic improvement in the magnitude of the β to R_{SB} ratio for a given base thickness, and also shows a qualitative shift in the functional behavior of the ratio to be much less dependent on base thickness. This improvement can be attributed to the reduction in carrier transit time due to the field induced by the graded base.

The InP/InGaAs HBTs used in this work were grown by low-pressure MOCVD using the graded-base growth technique. The key features of the epitaxial structure are an 800 Å InGaAs emitter cap ($n = 5\times10^{18}$ cm^{-3}), an 800 Å InP emitter ($N = 5\times10^{17}$ cm^{-3}), a 600 Å C-doped graded base ($p = 1.8\times10^{19}$ cm^{-3}), a 2500 Å InGaAs collector ($n = 1\times10^{16}$ cm^{-3}), and finally a 5000 Å InGaAs sub-collector ($n = 5\times10^{18}$ cm^{-3}). The Carbon concentration in the base is relatively low because of difficulties achieving a large concentration of activated acceptors due to Hydrogen passivation.

FABRICATION

Self-aligned high-frequency devices in a standard double-mesa design were fabricated using both e-beam and contact lithography, standard lift-off techniques for metalizations, and all wet chemical etching. The first step in the process flow was the deposition of a hexagonal-shaped emitter electrode and two terminal contacting posts: one each for the base and collector. Subsequent etching and metal deposition steps are manipulated so that after the front end processing, the two terminal posts are electrically continuous with the base and collector terminals. This enables a via-free contact between the device and an overlay metal deposition following planarization. E-beam lithography was used to define the pattern for this step, and relatively thick TiPtAu (150 Å, 150 Å, and 5500 Å) was evaporated. Emitter widths ranged from 3 μm to 0.3 μm, and emitter lengths of 16, 12, 5, and 4 μm were fabricated.

Undercutting beneath the emitter electrode during a self-aligned wet emitter etch is controlled to approximately 0.05 μm with the aid of a thin emitter cap epitaxial design. The self-aligned base metal is next defined using electron beam lithography. In this work the TiPtAu base metal is made very thin to avoid short-circuiting to the emitter metal; layer thicknesses of 100 Å, 150 Å, and 850 Å are used. The base terminal post is connected to a hexagonal-shaped base electrode by thin strip of metal, which is called a μ-bridge in this work.

During the wet base-collector etch, photoresist is used to protect the semiconductor layers beneath the emitter electrode as well the semiconductor surrounding the terminal posts, but the dimensions of the base-collector mesa are defined solely by the base electrode. The TiPtAu collector metal pattern is defined using contact lithography. Following a sintering step, an isolation etch is performed. During the isolation etch, the base terminal post is isolated from the active transistor by etch undercutting, leaving only the metal μ-bridge to connect the base terminal post to the active transistor. Figure 2 is an SEM picture of a transistor after front-end processing. The process is completed with planarization using BCB, an etch-back to expose the emitter electrode and terminal posts, and deposition of overlay metallization for ground-signal-ground RF probing.

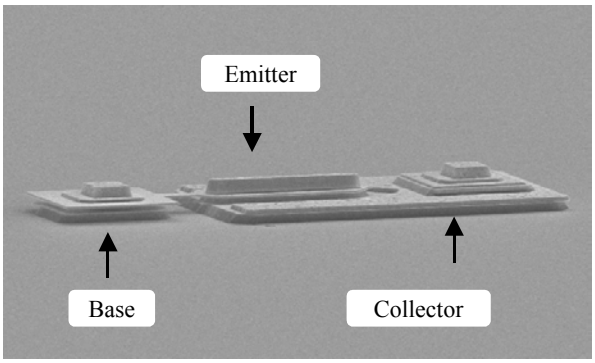

Fig. 2. A fabricated InP/InGaAs HBT before planarization

DEVICE RESULTS

Typical Gummel plots of fabricated HBTs with a 2 μm and 0.5 μm emitter width are shown in Fig. 3. The collector and base ideality factors determined at 0.5 V for both devices are 1.15 and 1.24, respectively.

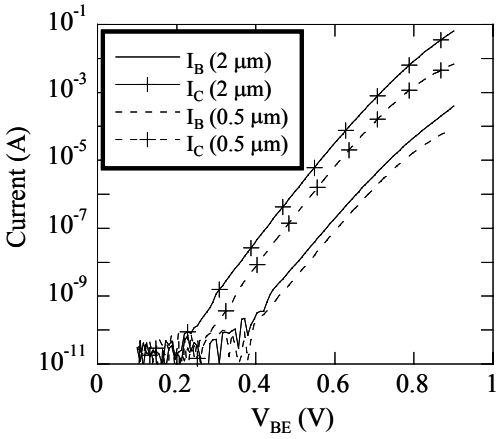

Fig 3. Gummel plots for two fabricated devices. The emitter length of both devices was 12 μm

.

The collector-emitter offset voltage $V_{CE,offset}$ is approximately 0.2 V, the knee voltage is less than 0.8 V, and the common-emitter breakdown voltage BV_{CEO} is approximately 2.2 V. These results indicate that these sub-micron HBTs are well suited for low-voltage, low power applications. The DC current gain β for the HBTs in this work decreased with emitter area as shown in Fig. 4. A decrease in β with emitter dimensions for an HBT is typically

attributed to an increase in the importance of parasitic base recombination currents with increasing perimeter-to-area ratio. Since InGaAs has a low surface recombination current, the decrease shown here is tentatively attributed to recombination at the base contact itself.

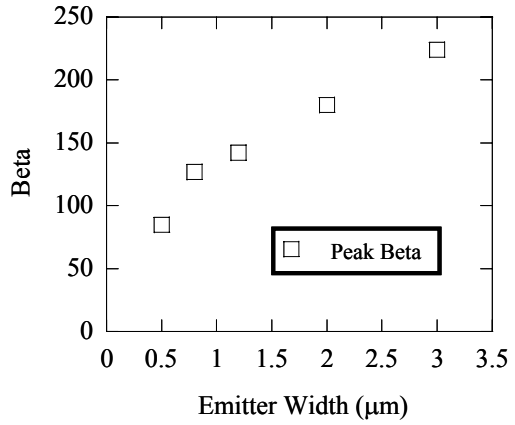

Fig 4. The decrease in β with emitter width. The emitter length of all devices was 12 μm

S-parameters were measured from 0.25 to 40 GHz using an HP8510C Network Analyzer. Off-wafer calibration was performed and y-parameters of open-pad structures were de-embedded. The cutoff frequencies f_T and f_{MAX} are calculated by extrapolating to unity at 20 dB/decade. Example extrapolation of $f_T = 205$ GHz and $f_{MAX} = 175$ GHz for a 0.5×8 μm^2 HBT are shown in Fig. 5.

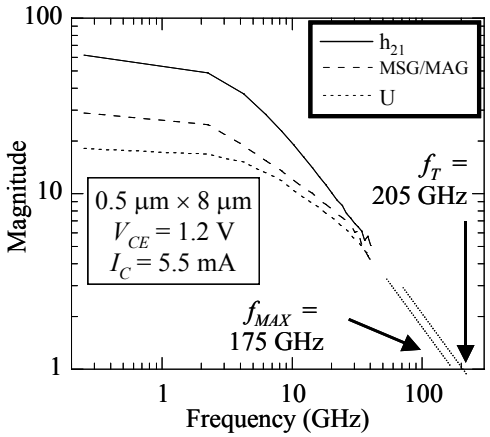

Fig 5. Example extrapolation of f_T and f_{MAX}

RF performance data for different size devices are shown in Fig. 6. These results show that f_{MAX} is inversely proportional to the inverse square root of emitter width for devices as small as 0.5 μm. This relationship is in accordance with the idealized scaling relationship for small-area transistors. Our data also show a significant increase in f_T with decreasing emitter width, a result in opposition to standard theory of bipolar transistor scaling. This trend may be in part attributable to a reduction in device self-heating as device size is reduced. Figure 7 shows area-normalized thermal resistance for different sized devices. The normalized thermal resistance and operating junction temperature are much smaller for small area devices.

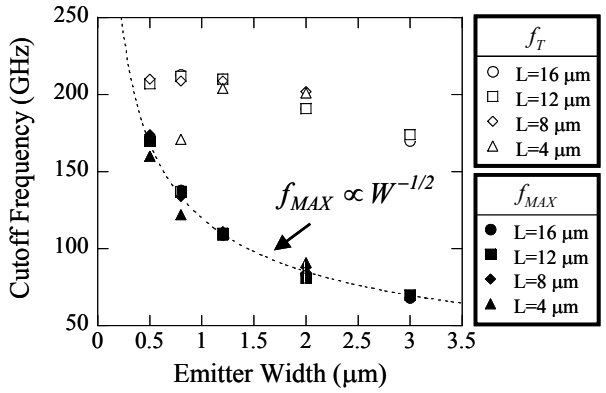

Fig 6. RF performance scaling data

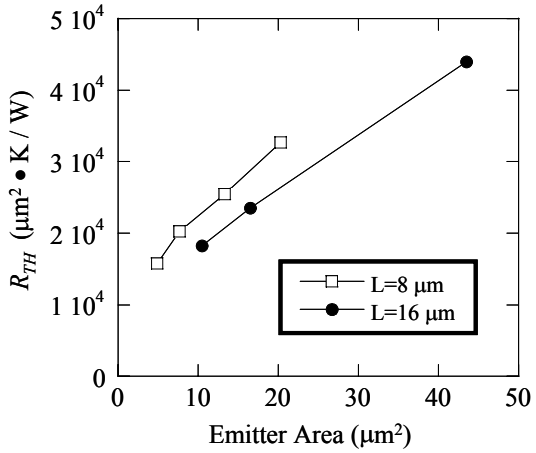

Fig 7. Area-normalized thermal resistance for different sized devices.

The possibility finite resistance of the gold μ-bridge negatively impacting device performance was investigated by fabricating devices with bridge widths of 0.5 μm, 0.8 μm, and 1.2 μm and measuring the RF performance of the transistors. The results of this experiment are shown in Fig. 8. Fig. 8 demonstrates that any negative impact of the μ-bridge on HBT performance must be minor because there is no obvious trend in the RF performance as the bridge width changes.

The reduced sum $f_T \times f_{MAX} \div (f_T + f_{MAX})$ has been suggested as a single figure of merit that can be used to compare different transistor technologies. [8] Figure 9 shows this term for several published InP-based HBTs as a function of base doping level. Although the base doping level of the transistors in this work was a modest 1.8×10^{19} cm^{-3}, the transistor performance is comparable to that of transistors

with base doping as high as 4×10^{19} cm^{-3}, a result which the authors attribute to the small emitter width and careful control of parasitics.

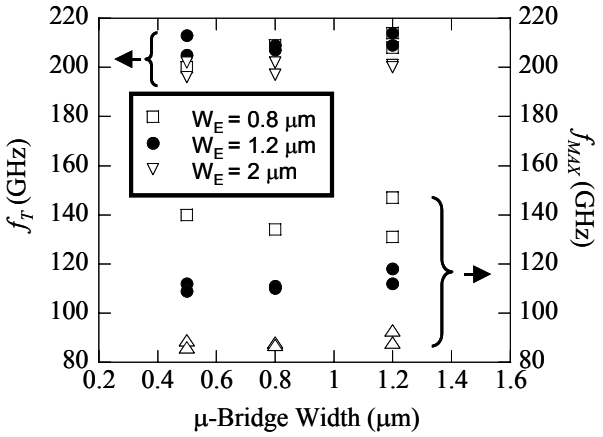

Fig 8. RF performance vs. μ-bridge width. The emitter length of all devices was 12 μm.

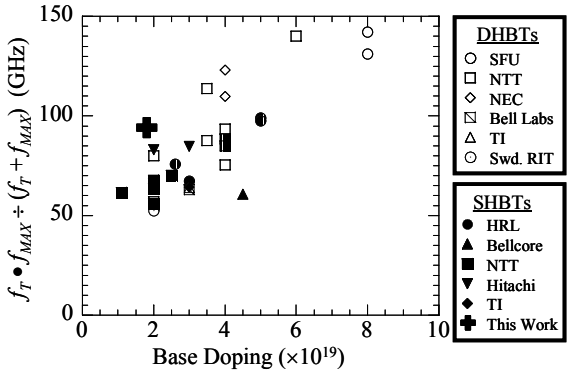

Fig 9. InP HBT RF performance measured with a single parameter derived from f_T and f_{MAX} vs. base doping in technical literature.

CONCLUSIONS

This paper has demonstrated excellent RF characteristics in an InP/InGaAs SHBT grown by MOCVD with a base doping level of 2×10^{19}. The epitaxial structure incorporated a compositionally-graded base and the fabrication process utilized aggressive lateral scaling and control of parasitics. The DC current gain β decreases rapidly with emitter width, but is still at a reasonable level for devices with emitter widths as small as 0.5 μm. The f_{MAX} data showed ideal increases with the inverse square root of emitter width down to 0.5 μm.

ACKNOWLEDGMENT

This work was partially supported under NSF ECS-9979341. Mike Hattendorf wishes to acknowledge the support of the Fannie and John Hertz Foundation through a Hertz Fellowship. The authors also extend gratitude to Nada El-Zein and David Becher for useful discussions.

REFERENCES

[1] S. Bahl, N. Moll, *et. al.*, "Be diffusion in InGaAs/InP heterojunction bipolar transistors," IEEE Electron Dev. Lett. **21**, 332-334, July 2000.

[2] R. Malik *et. al.*, "Self-aligned thin emitter C-doped base InP/InGaAs/InP DHBT's for high speed digital and microwave IC applications," 54th Annual Device Research Conference Digest, 40-41, 1996.

[3] H-C Kuo, *et. al.*, "Growth of carbon doping Ga/sub 0.47/In/sub 0.53/As using CBr_4 by gas source molecular beam epitaxy for InP/InGaAs heterojunction bipolar transistor applications," AIP for American Vacuum Soc. Journal of Vacuum Science & Technology B **17**, 1185-1189, June, 1999.

[4] M. Ida *et. al.*, "InP/InGaAs DHBTs with 341 GHz fT at high current density of over 800 kA/cm^2," Proceedings of the 2001 IEEE Electron Devices Meeting.

[5] H. Ito, S. Yamahata, N. Shigekawa, and K. Kurishima, "High f_{MAX} carbon-doped base InP/InGaAs heterojunction bipolar transistors grown by MOCVD," Electronics Letters, **32**, 1415-1416, July 1996.

[6] M. Sokolich, C.H. Fields, and M. Madhav, "Submicron AlInAs/InGaAs HBT with 160 GHz f_T at 1 mA," IEEE Electron Dev. Lett. **22**, 8-10, January 2001.

[7] Bipul Agarwal, Ph.D. dissertation. University of California at Santa Barbara, 1998.

[8] A. Fujihara, *et. al.*, "High-Speed InP/InGaAs DHBTs with ballistic collector launcher structure," Proceedings of the 2001 IEEE Electron Devices Meeting.

ACRONYMS

HBT: Heterojunction Bipolar Transistor
MOCVD: Metal-Organic Chemical Vapor Deposition
MBE: Molecular Beam Epitaxy
SHBT: Single Heterojunction Bipolar Transistor
DHBT: Double Heterojunction Bipolar Transistor
RF: Radio Frequency
DC: Direct Current
SEM: Scanning Electron Microscope
BCB: Benzocyclobutene